Numerical Simulations of a Cycloidal Wave Energy Converter

Jürgen Seidel[1,#], Casey Fagley[1] and Stefan Siegel[1]

1 Atargis Energy Corporation, 3185 Janitell Road Ste 101
Corresponding Author / E-mail: Jurgen.Seidel@Atargis.com, TEL: +1-719-214-8815 x201

KEYWORDS : Cycloidal Wave Energy Converter

A simulation methodology for a Cycloidal Wave Energy Converter is presented. Expanding on earlier simulations, the hydrofoils are now modeled using a panel method to discretize the hydrofoil surface. Standard panel method techniques are used to enforce tangential flow on the hydrofoil and also to ensure the Kuttal condition is satisfied. The code is validated using a deeply submerged CycWEC with a large radius so that standard airfoil simulations could be used for comparison. In addition to the nearly linear motion, at large depths the influence of the free surface decreases rapidly. Simulations of an experimentally tested Cycloidal Wave Energy Converter show that hydrofoil curvature, used to account for the circular motion of the hydrofoil on a Cycloidal Wave Energy Converter, the surface pressure distribution on the hydrofoil changes significantly when compared to a standard hydrofoil in uniform flow. When the Cycloidal Wave Energy Converter is brought close to the free surface, cyclical variations of the pressure distribution during a revolution of the hydrofoil were observed.

NOMENCLATURE

c = x+iy location in the complex plane
c = hydrofoil chord length
c_p = Pressure coefficient
g = Gravity constant
k = Wave Number
p = Pressure
p_∞ = Reference static pressure
q_∞ = Reference dynamic pressure
R = CycWEC Radius
t = Time
T = Wave Period
u,v = Velocity components in the x-, y-directions
x = horizontal coordinate
y = vertical coordinate
y_c = Submergence depth of WEC shaft
z=x+iy complex coordinate
α = Angle of attack
Γ = Circulation
Φ = Velocity potential
Ψ = Stream function
η = Surface elevation

1. Introduction

Ocean waves have a tremendous potential to provide clean renewable energy. In comparison to other renewable energy sources, wave power has many benefits, including global availability, high predictability and consistency, and co-location with densely populated areas. In addition, the energy density compared to solar and wind is much higher, resulting in a dramatically reduced device size (and therefore cost) necessary to harvest a given amount of energy. Even though all these positive factors of wave power have been known for quite a while, current technologies have not been able to efficiently harness this energy. A number of reasons can be identified. First, most wave energy devices in development today use buoyancy or drag as the primary force exerted by the waves on the device to extract energy. Because of this interaction mechanism, these devices, characterized as oscillating point absorbers, are bounded by first principle considerations to a 25% maximum efficiency; similarly, drag based

devices experience a substantial decrease in the efficiency. With this limitation, the device size has to be very large to extract appreciable amounts of energy from the waves. Second, these large devices experience enormous structural loads during operation, but in particular during storms. And finally, because the oscillatory motion has to be converted to rotational shaft power, current devices require power take off systems, which incur additional losses. These unsolved engineering issues have at large prevented utility scale wave power production.

A cycloidal wave energy converter (CycWEC) is a novel design which addresses these engineering issues (see Figure 1). The CycWEC uses lift based hydrofoils as a means of interacting with ocean waves as well as feedback control to adjust to the incoming waves. A lift based device allows for much larger efficiency as well as the ability to feather in the case of extreme sea states. In addition, the device is fully submerged and the submergence depth can be increased to mitigate the harmful interactions with storm seas. Finally, a CycWEC produces shaft power directly, thus eliminating the need for a complex power take off system.

The CycWEC in a two-dimensional wave flume acts as a wave termination device and thus has a theoretical inviscid efficiency limit of 100%. Inviscid numerical simulation have shown efficiencies upwards of 99% in both harmonic wave extraction as well as irregular sea states [1,2]. 1:300 model scale testing in both harmonic and irregular sea states result in efficiencies over 80% [2,7].

In this paper, an improved simulation code is presented where the hydrofoils of the CycWEC are modeled as true hydrofoils and not as individual vortices with a given circulation Γ (see Figure 1) as in earlier simulations [9].

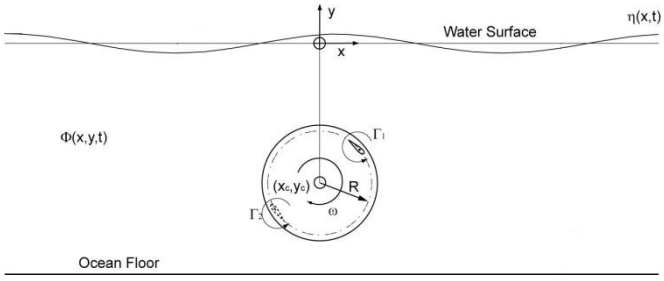

Figure 1: CycWEC sketch.

2. Simulations

The CycWEC and wave-induced flow field is modeled using potential flow theory. For an inviscid, incompressible, and irrotational flow, the governing continuity equation simplifies to the Laplace equation,

$$\nabla^2 \Phi = 0,$$

where Φ is the velocity potential. Unique solutions to this equation are determined by satisfying the appropriate boundary conditions based on physical considerations. For two-dimensional problems, it is convenient to define the complex stream function in terms of the complex coordinate $z = x + iy$

$$F(z,t) = \Phi + i\Psi,$$

where $\Psi(z,t)$ is the stream function and the complex velocity is defined by $dF/dz = u - iv$.

2.1 Cycloidal Wave Energy Converter Model

Following standard panel methods, the hydrofoils of the CycWEC can be modeled as a series of vortices located on panels on the surface of the hydrofoil. However, for hydrofoils in proximity to a free surface, care has to be taken to account for the effect of the free surface. In the panel method, these effects are included in the forcing vector of the influence matrix system.

The derivation of the linearized free surface boundary condition can be found e.g. in [8]. Neglecting higher order terms, the kinematic boundary condition ensuring the vertical velocity of the free surface and the fluid are equal is

$$\frac{\partial \eta}{\partial t} = \frac{\partial \Phi}{\partial y}.$$

The dynamic boundary condition ensuring the pressure on the free surface is atmospheric is determined from Bernoulli's equation. Substituting the free surface elevation for y, and again neglecting higher order terms yields

$$\eta = -1/g \frac{\partial \Phi}{\partial t}$$

where g = 9.81 m/s is the gravity constant. Due to the linearization, Equation 4 can be imposed at y = 0. A non-reflective boundary condition is applied at the domain boundaries to avoid wave reflections.

Subject to the above boundary conditions, the complex potential for a vortex moving under a free surface at position $c(t) = x(t) + iy(t)$ in the complex plane is developed in [9],

$$F(z,t) = \frac{\Gamma(t)}{2\pi i} \ln\left[\frac{z - c(t)}{z - \bar{c}(t)}\right] + \frac{g}{\pi i}\int_0^t \int_0^\infty \frac{\Gamma(\tau)}{\sqrt{gk}} e^{-ik(z-\bar{c}(\tau))} \sin\left[\sqrt{gk}(t-\tau)\right] dk\, d\tau$$

where Γ(t) is the circulation of the vortex, and k the wave number. The first term is the complex potential due to the vortex and its mirror image above the surface, which is necessary to satisfy the kinematic free surface condition. The second term describes the radiated waves related to the dynamic free surface condition. Note that the fluid is assumed to be infinitely deep.

Each CycWEC hydrofoil is modeled by numerically integrating the equation above using a second order time and wave number marching technique. To ensure that the numerical solution converges, numerical

integration settings for Δt, Δk, and k_{max} were chosen based on the results of the convergence study presented in [1]. The dynamic boundary condition is then used to compute the surface elevation and wave pattern.

The theory of superposition is used to extend this approach to compute a CycWEC where the hydrofoils are modeled using panels and the total potential is determined as $\Phi_{total} = \sum_{i=1}^{N} \Phi_i$ where Φ_i is the potential of a single vortex. To enforce the Kutta condition of tangential flow at the trailing edge, standard panel method techniques are followed.

2.2 Cycloidal Wave Energy Converter Motion

The motion of a hydrofoil of the Cycloidal Wave Energy Converter is defined by the submergence depth y_c, the CycWEC radius R, and the rotational period T. With these quantities, the hydrofoil velocity magnitude becomes $U = 2\pi R/T$.

4. Results

4.1 Validation

To approximate the conditions of a standard panel code, i.e. a uniform free stream velocity, the CycWEC radius was set to R=1000m and the submergence depth to y_c=1500m. Therefore, at the bottom of the motion path, the hydrofoil is submerged at y=2500m. While no detailed study of the influence of the free surface was performed for these simulations, earlier results indicated that a depth y_c>10m is sufficient. The large radius was chosen so as to approximate a linear motion, which is kinematically equivalent to a uniform free stream. Geometrical considerations show that in the motion segment considered in the validation simulations, the angle of attack changes by less than 0.01°, approximating a linear movement very well. The simulations converged in less than 20 iterations. Unless otherwise noted, the simulations were performed using 80 panels on the hydrofoil surface.

4.1.1 Symmetric hydrofoil

The first test of the newly developed simulation code was performed using a NACA0015 hydrofoil. The hydrofoil is shown in Figure 2.

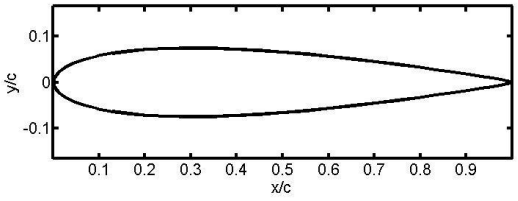

Figure 2: NACA0015 geometry.

Figure 3 shows a comparison of data obtained from Javafoil [10] with the data from the new code. The figure shows the pressure coefficient $c_p = (p - p_\infty)/q_\infty$, where p_∞ is the reference static pressure and $q_\infty = 1/2\rho U_\infty^2$ is the reference dynamic pressure. Data at angles of attack of $\alpha = 0°, 6°, \text{and } 10°$ are plotted. Good agreement of the pressure distribution is achieved. The slight differences in the suction side pressure distribution are due to slightly different panel distribution and the fact that Javafoil uses a linear vorticity distribution on the panels while the current code uses a constant vorticity value for each panel. Due to the symmetry of the hydrofoil, only positive angles of attack have been computed.

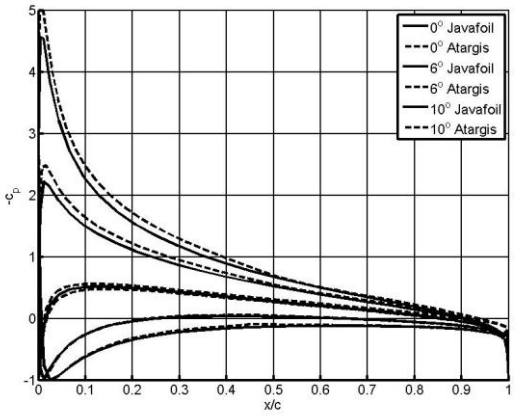

Figure 3: NACA0015 hydrofoil. Comparison of pressure coefficient on the hydrofoil surface between Javafoil and Atargis.

4.1.2 Asymmetric hydrofoil

In order to test the simulation code for an hydrofoil that creates lift at $\alpha = 0°$ angle of attack, simulations have been performed using a NACA4412 hydrofoil. The hydrofoil contour is plotted in Figure 4.

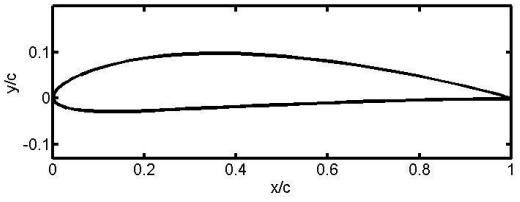

Figure 4: NACA4412 hydrofoil.

Note that for an asymmetric hydrofoil, i.e. a hydrofoil with camber, the lift is nonzero at zero angle of attack. A comparison of the pressure distribution at angles of attack $\alpha = 0°, 6°, \text{and } 10°$ with the results obtained using Javafoil is shown in Figure 5.

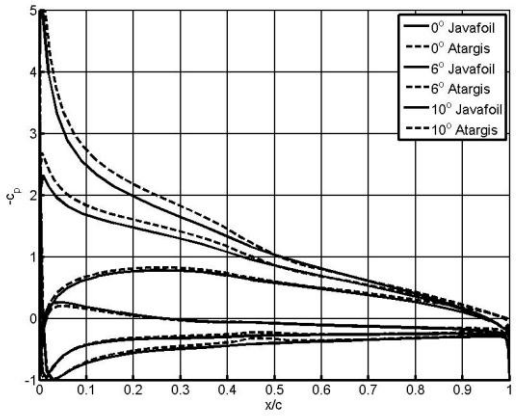

Figure 5: NACA4412 hydrofoil. Comparison of pressure coefficient on the hydrofoil surface between Javafoi and Atargis.

Overall, good agreement is achieved. At $\alpha=0^o$, both the suction and pressure side c_p distribution are in very good agreement with the results obtained by Javafoil. As the angle of attack is increased, the newly developed code computes a slightly lower pressure on the suction side, while the pressure side cp distribution remains in very good agreement with the Javafoil data. This is most likely caused by the difference in the discretization schemes; Javafoil uses a linearly varying circulation over each panel while the Atargis code assumes a constant circulation. To improve the predictions, more panels would have to be added to the suction side of the hydrofoil. However, the level of prediction accuracy using the current discretization was determined to be adequate for the current investigation.

4.2 CycWEC simulations

With the code validated for standard hydrofoils, simulations were performed for the geometry of a 1:10 CycWEC tested experimentally [11]. This CycWEC has a radius R=1m and the hydrofoils are designed from the NACA0015 hydrofoil. To compensate for the circular motion of the CycWEC, the hydrofoil chord is curved such that at $\alpha=0^o$ angle of attack, the chord is aligned with the circle along which the blade travels (Figure 6). The design chord length is c=0.75m.

For simplicity, data for only one hydrofoil is computed here. The waves generated (or cancelled) by a CycWEC with two blades can be computed from this data using the method of superposition. In a typical setup, one blade of the CycWEC is pitched at a positive angle of attack (nose outward) while the other blade is pitched at the same angle inward, i.e. in the negative direction. Earlier simulations and experiments have shown that this configuration results in the best one-sided wave generation and therefore also the best wave cancellation [1,2,9].

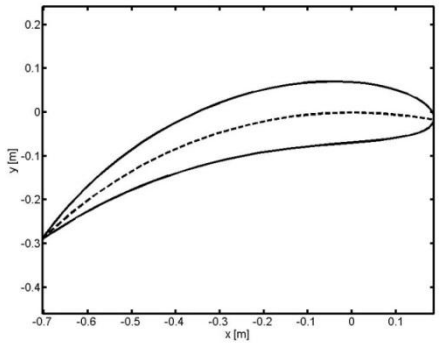

Figure 6: Curved NACA0015 hydrofoil geometry. Dashed line indicates blade chord and path of travel ($\alpha=0^o$).

4.2.1 Deep submergence

For a deeply submerged hydrofoil (y_c=1500m, R=1000m), the free surface does not have a significant influence on the pressure distribution. However, the curved hydrofoil in conjunction with the rotational motion results in a significant change in the pressure distribution around the hydrofoil (Figure 7). As the figure shows, the curved hydrofoil rotating around the main shaft of the CycWEC reaches the same low pressure at the suction peak near the leading edge as the straight hydrofoil in linear motion. However, the pressure on the suction side remains at lower levels and at higher levels on the pressure side, resulting in significantly larger lift.

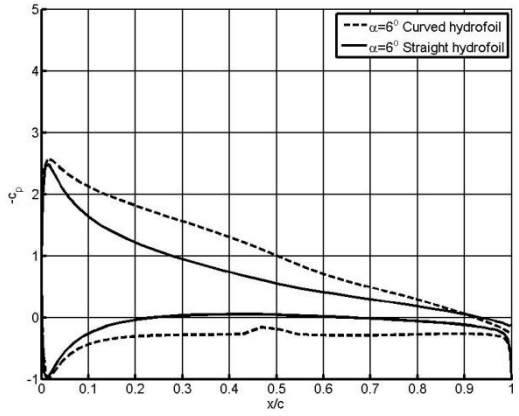

Figure 7: Comparison of pressure distribution of curved and straight hydrofoil. $\alpha=6^o$.

4.2.2 CycWEC conditions

To simulate the waves generated by CycWEC at the experimental CycWEC conditions [11], the CycWEC main shaft was submerged y_0=1.5m. With the CycWEC radius R=1m and the hydrofoil chord of c=0.75m, the geometry shown in Figure 8 results. The blade at the top of the figure as an angle of attack of $\alpha=+6^o$.

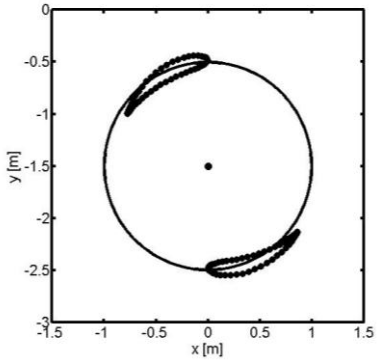

Figure 8: CycWEC with two blades, angle of attack $\alpha=\pm 6°$.

The pressure distributions for the positively and negatively pitched hydrofoils are shown in Figure 9 and Figure 10, respectively, and compared to the results obtained from Javafoil.

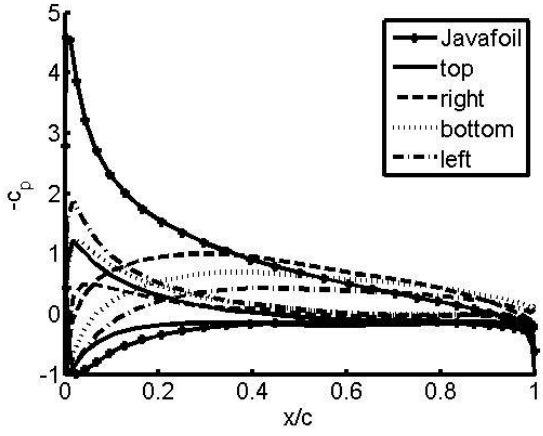

Figure 9: Pressure distribution on curved NACA0015 hydrofoil. $\alpha=+6^{o}$.

In the figure, the surface pressure distribution is plotted when the hydrofoil is at the top, right, bottom, and left in the CycWEC revolution. The data shows that even at the bottom of the revolution, where the hydrofoil is the furthest away from the free surface (y_c=2.5m), the pressure distribution does not approach the one predicted by Javafoil for a hydrofoil in a uniform free stream. It is interesting to note that even at the left and right positions, the pressure distribution differs significantly. This is mainly due to the large chord to radius ratio, which results in significantly different submergence depths in these two positions (see Figure 8 for a representation of the hydrofoil in two different positions for a size comparison).

When the data for the positively and negatively pitched hydrofoil is compared (Figure 9 and Figure 10, respectively), only very minor changes in the pressure distribution were observed. Note that the role of the pressure and suction sides are now reversed, i.e. the suction side of the hydrofoil for a negative pitch angle faces the center of rotation.

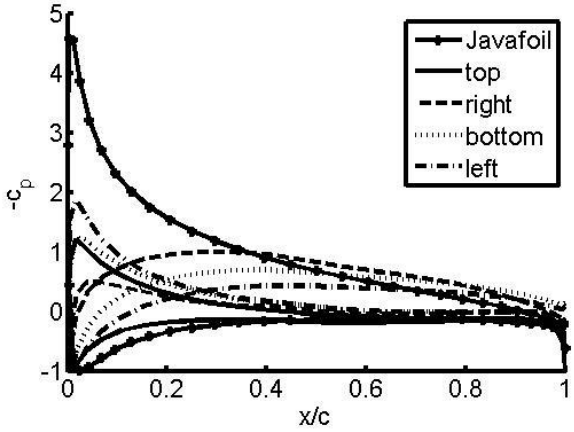

Figure 10: Pressure distribution on curved NACA0015 hydrofoil. $\alpha=-6^{o}$.

CONCLUSIONS

An extension of a simulation code for computations of a Cycloidal Wave Energy Converter has been developed. While in earlier versions, the hydrofoils of the CycWEC were represented by a single vortex with specified circulation Γ, the newly developed code allows for modeling the hydrofoils using a panel method. In the numerical method, the hydrofoils are represented by a number of panels with constant circulation. Care has been taken to satisfy the Kutta condition on the hydrofoil.

Validation simulations have been performed for deeply submerged hydrofoils. This allowed for comparison with standard airfoil panel codes such as Javafoil. For both symmetric and cambered hydrofoils, very good agreement of the pressure distribution results has been achieved.

When the CycWEC hydrofoil was simulated for the experimentally tested conditions, significant changes in the pressure distribution were observed. Due to the proximity of the free surface, the minimum pressure on the suction side was greatly reduced. Interestingly, positive and negative pitch angles show virtually identical pressure distributions.

ACKNOWLEDGEMENTS

The authors would like to acknowledge fruitful discussion with Dr. Tiger Jeans. This material is based upon work supported by the Department of Energy under Award Number DEEE0003635.

Disclaimer

that its use would not infringe privately owned rights. Reference herein to any specific commercial product, process, or service by trade name, trademark, manufacturer, or otherwise does not necessarily constitute or imply its endorsement, recommendation, or favoring by the United States Government or any agency thereof. The views and opinions of authors expressed herein do not necessarily state or reflect those of the United States Government or any agency thereof.

REFERENCES

[1] S. G. Siegel, T. L. Jeans, and T. E. McLaughlin, "Deep ocean wave energy conversion using a cycloidal turbine," Applied Ocean Research, vol. 33, no. 2, pp. 110–119, 2011.

[2] S. G. Siegel, T. L. Jeans, and T. E. McLaughlin, "Intermediate ocean wave termination using a cycloidal wave energy converter," in Proceedings of 29th International Conference on Ocean, Offshore and Artic Engineering, no. OMAE2010-20030, Shanghai, China, 2010.

[3] J. Pinkster and A.J.Hermans, "A rotating wing for the generation of energy from waves," in 22nd IWWWFB Conference, Plitvice, Croatia, 2007.

[4] C. Marburg, "Investigation on a rotating foil for wave energy conversion," Master's thesis, TU Delft, 1994.

[5] A. J. Hermans, E. van Sabben, and J. Pinkster, "A device to extract energy from water waves," Applied Ocean Research Computational Mechanics Publications, vol. Vol. 12, No. 4, p. 5, 1990.

[6] E. van Sabben, "De in het snelheidsveld van lopende golven ronddraaiende plaat; invloed op het vrije vloeistofoppervlak," Master's thesis, TU Delft, 1987.

[7] S. G. Siegel, M. Roemer, J. Imamura, C. Fagley, and T. E. McLaughlin, "Experimental wave generation and cancellation with a cycloidal wave energy converter," in Proceedings of 30th International Conference on Ocean, Offshore and Artic Engineering, no. OMAE2011-49212, Rotterdam, The Netherlands, 2011.

[8] J. Wehausen and E. Laitone, Surface Waves, Handbook of Physics, Vol.9. Springer-Verlag, 1960.

[9] T. Jeans, S.G. Siegel, C. Fagley, and J. Seidel, "Irregular Deep Ocean Wave Energy Conversion Using a Cycloidal Wave Energy Converter", EWTEC2011, Southampton, Great Britain, 2011.

[10] M. Hepperle, Javafoil, http://www.mh-aerotools.de/airfoils /Javafoil.htm

[11] C. Fagley, S. Siegel, J. Seidel, "Wave Cancellation Experiments using a 1:10 Scale Cycloidal Wave Energy Converter," 1st AWTEC Conference, Jeju Island, Korea